

Reprogramming within hours following nuclear transfer into mouse but not human zygotes

Dieter Egli, Alice E. Chen, Genevieve Saphier, Claire Fitzgerald, Kathryn J. Go, Nicole Acevedo, Jay Patel, Manfred Baetscher, William G. Kearns, Robin Goland, Rudolph L. Leibel, Douglas A. Melton and Kevin Eggan

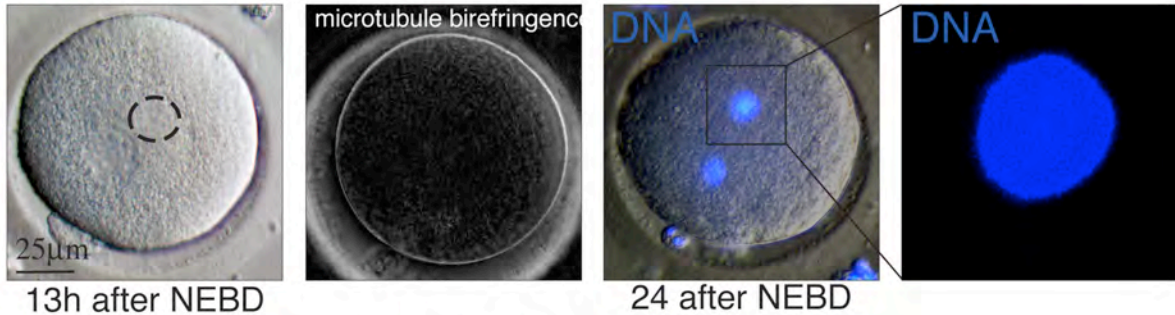
Content:

Supplementary Figures S1-S17

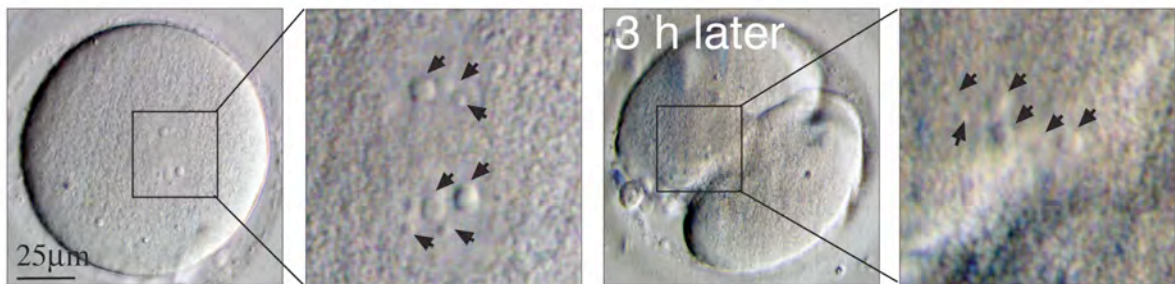
Supplementary Tables S1-S7

Supplementary Figures

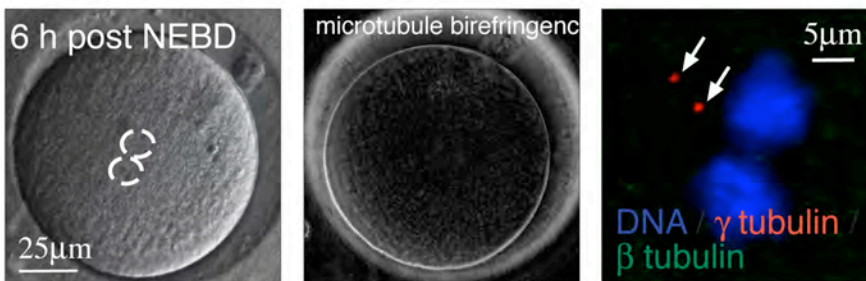
a Incomplete chromosome condensation



b Incomplete dissolution of nucleoli

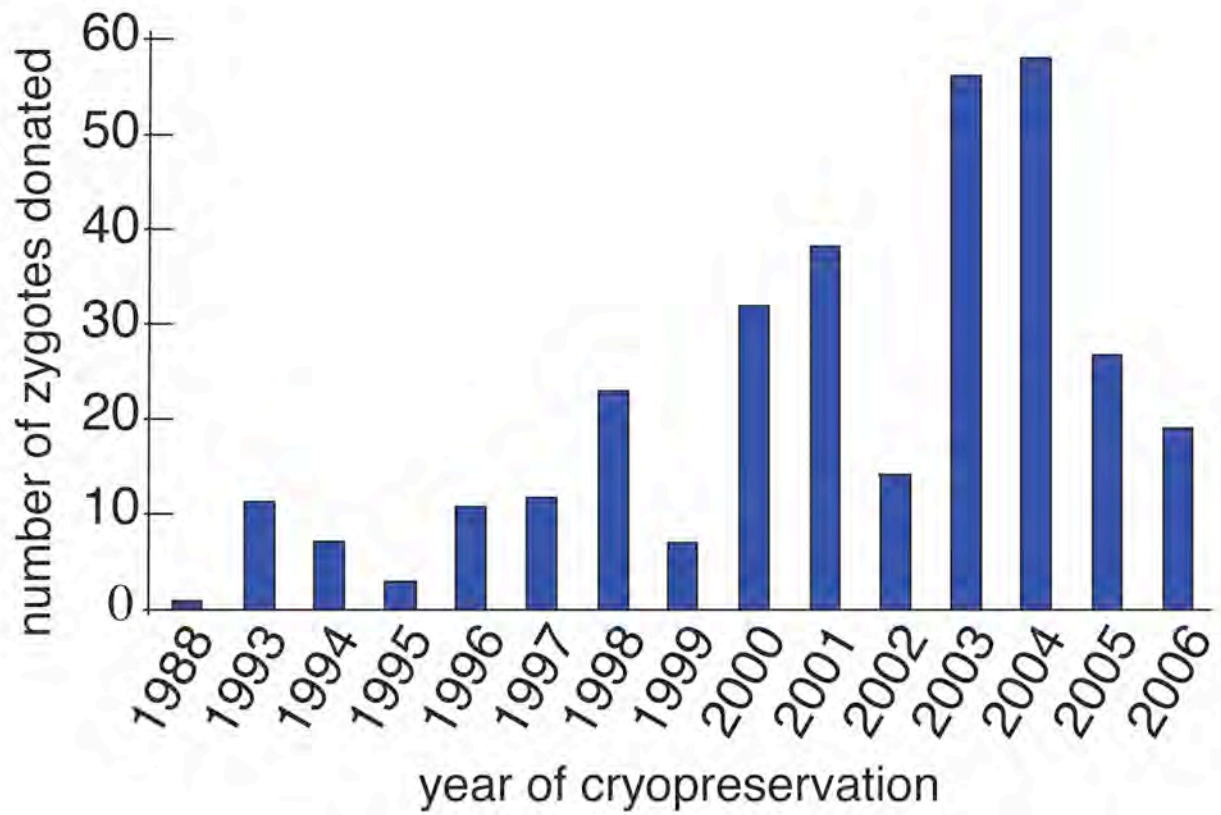


c Failure to assemble a spindle



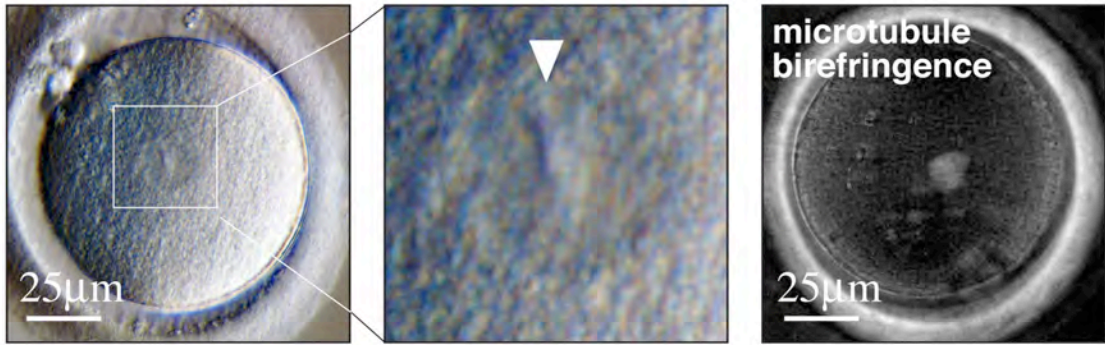
Supplementary Figure S1. Mitotic defects of cryopreserved human zygotes

a, zygote with asynchronous nuclear envelope breakdown and a failure to completely condense chromosomes. 13h post breakdown of the first nuclear envelope (circled), the second nuclear envelope is still intact. After 24h, both nuclear envelopes are broken down, but the chromosomes are not condensed. Absence of microtubule birefringence indicates failure to assemble a spindle. **b**, zygote that attempts (but ultimately fails) cleavage without completely dissolving the nucleoli. Both nuclear envelopes are broken down. Arrows point to nucleoli. **c**, Zygote arrested in mitosis. The two arrows point to the two γ tubulin marked centrosomes that normally nucleate a beta-tubulin positive spindle. NEBD = nuclear envelope breakdown.



Supplementary Figure S2. Human zygotes donated for research by year of cryopreservation

Shown is the number of zygotes donated to research obtained by year of cryopreservation.

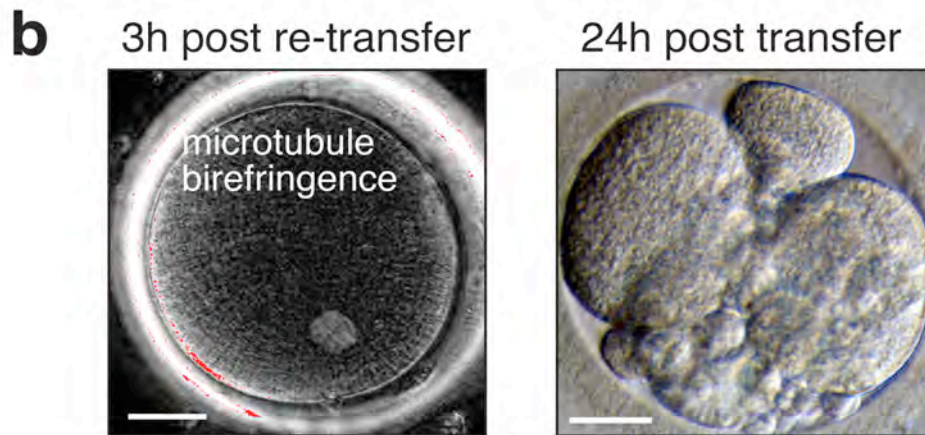
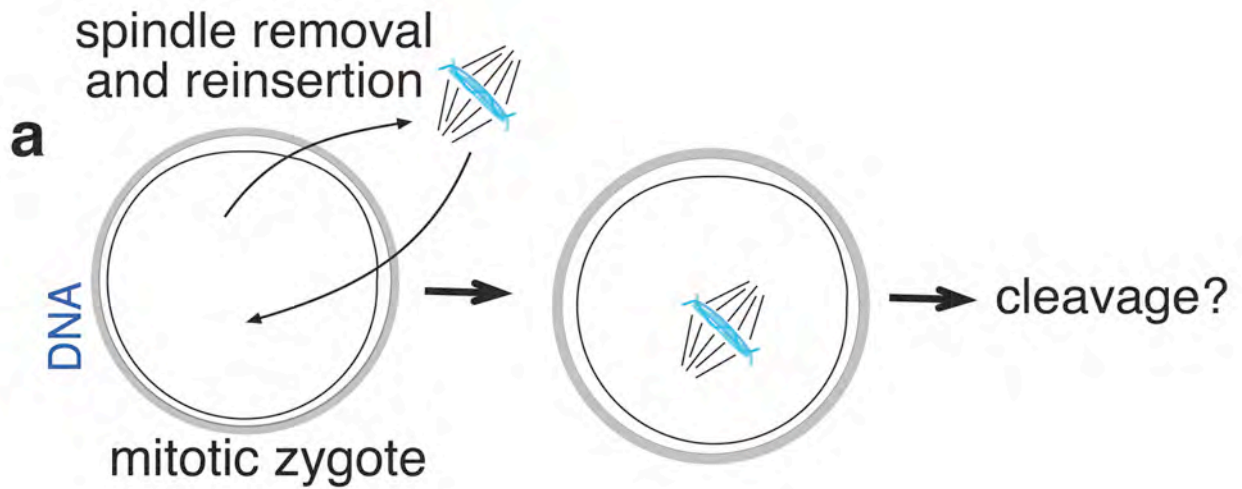


zygote frozen in mitosis
30min post thaw

spindle birefringence
30min after thaw

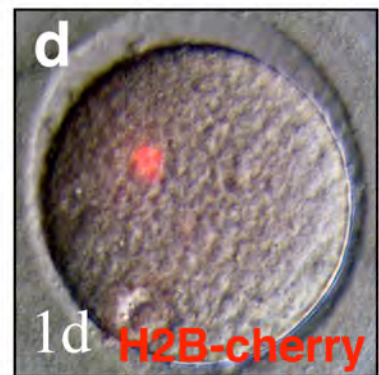
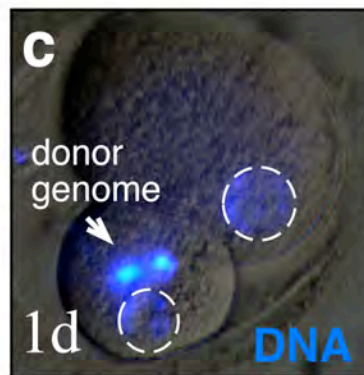
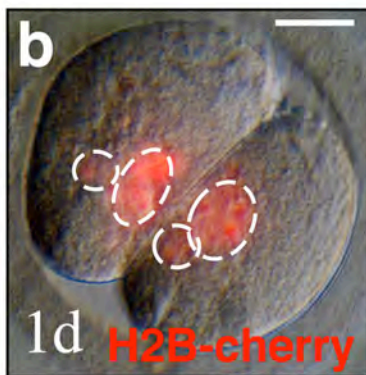
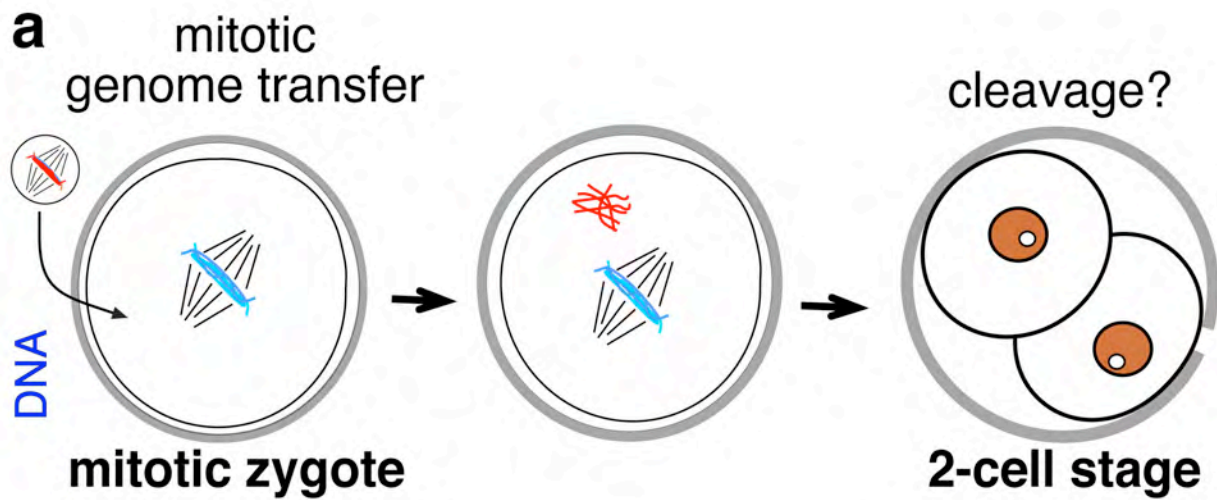
Supplementary Figure S3. Spindle assembly after cryopreservation of human zygotes in mitosis

Human zygote 30 minutes after thaw. The arrowhead points to the chromosomes at the metaphase plate. A birefringent spindle is present.



Supplementary Figure S4. Abnormal cleavage of human zygotes after spindle removal and re-transfer

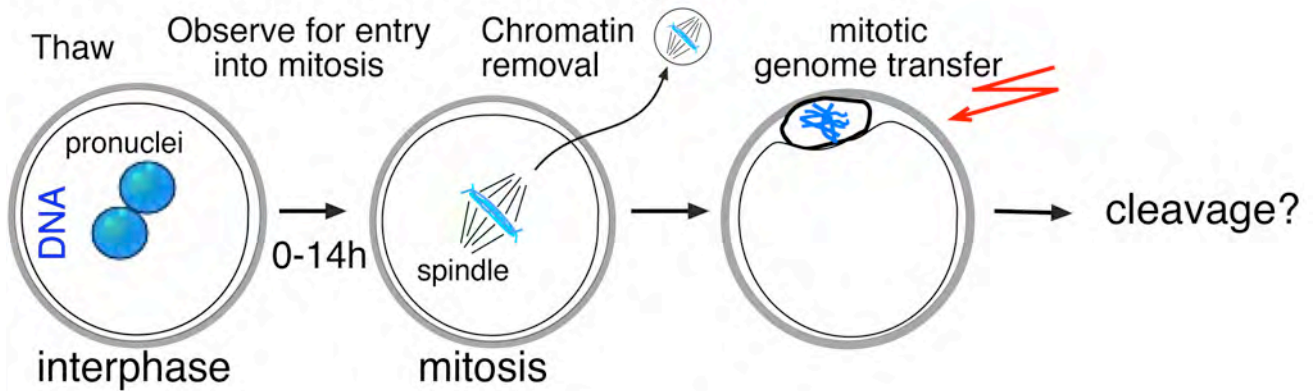
a, Schematic of the spindle removal and retransfer. **b**, zygote 3h post re-transfer, and after attempted cleavage. Scale bar: 25 μ m.



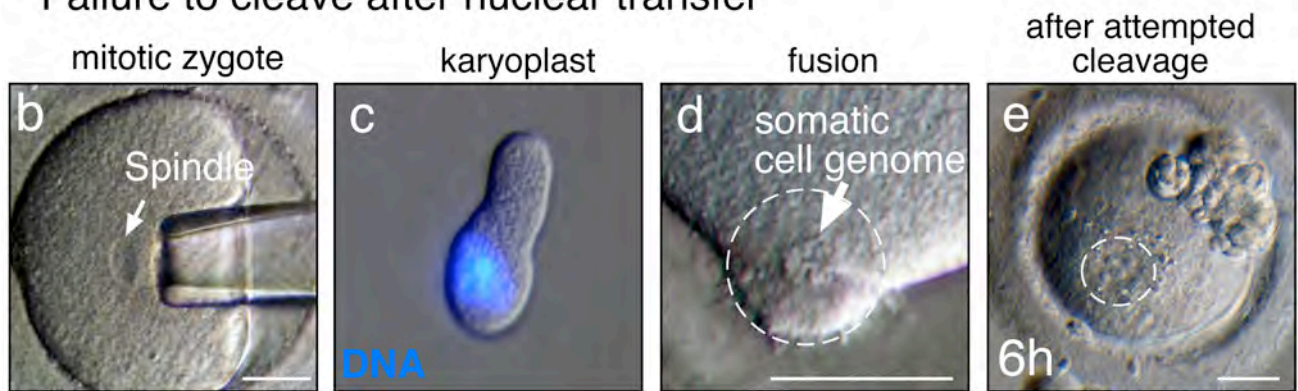
Supplementary Figure S5. Inefficient incorporation of donor chromatin into a spindle

a, Schematic showing the transfer of the somatic genome, but not the removal of the zygotic genome, resulting in a cell containing both genomes. **b-d**, 1 day after direct injection of a mitotic genome (red) into a zygote in mitosis without removal of the zygotic genome. **b**, Nuclei are circled. **c**, The arrow points to the injected genome, the endogenous zygotic genome is circled. **d**, H2B-cherry marked donor chromosomes were used, therefore the injected genome is marked by H2B-cherry, the zygote arrested in mitosis. Scale bar: 25 μ m.

a Nuclear transfer into human zygotes

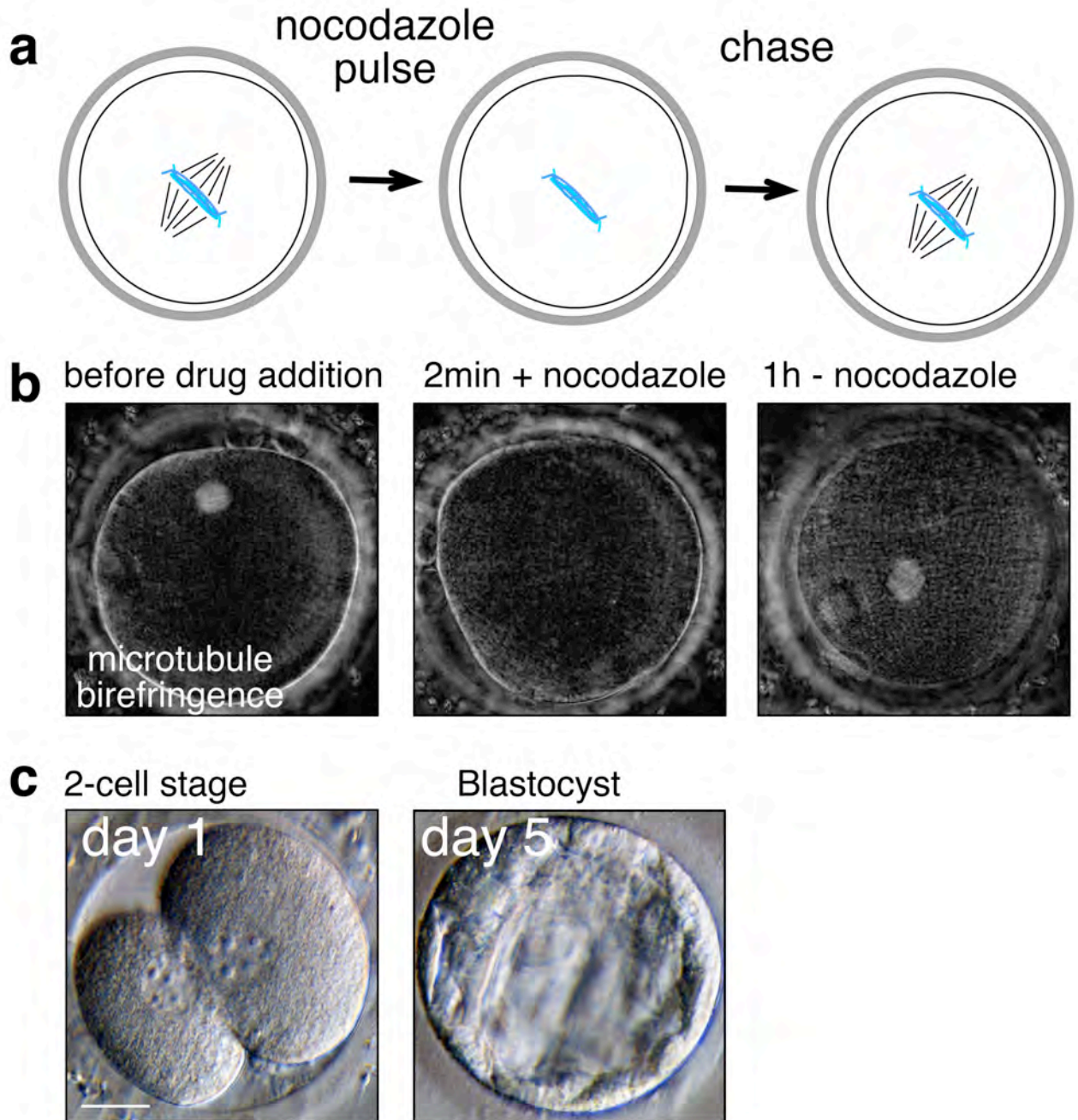


Failure to cleave after nuclear transfer



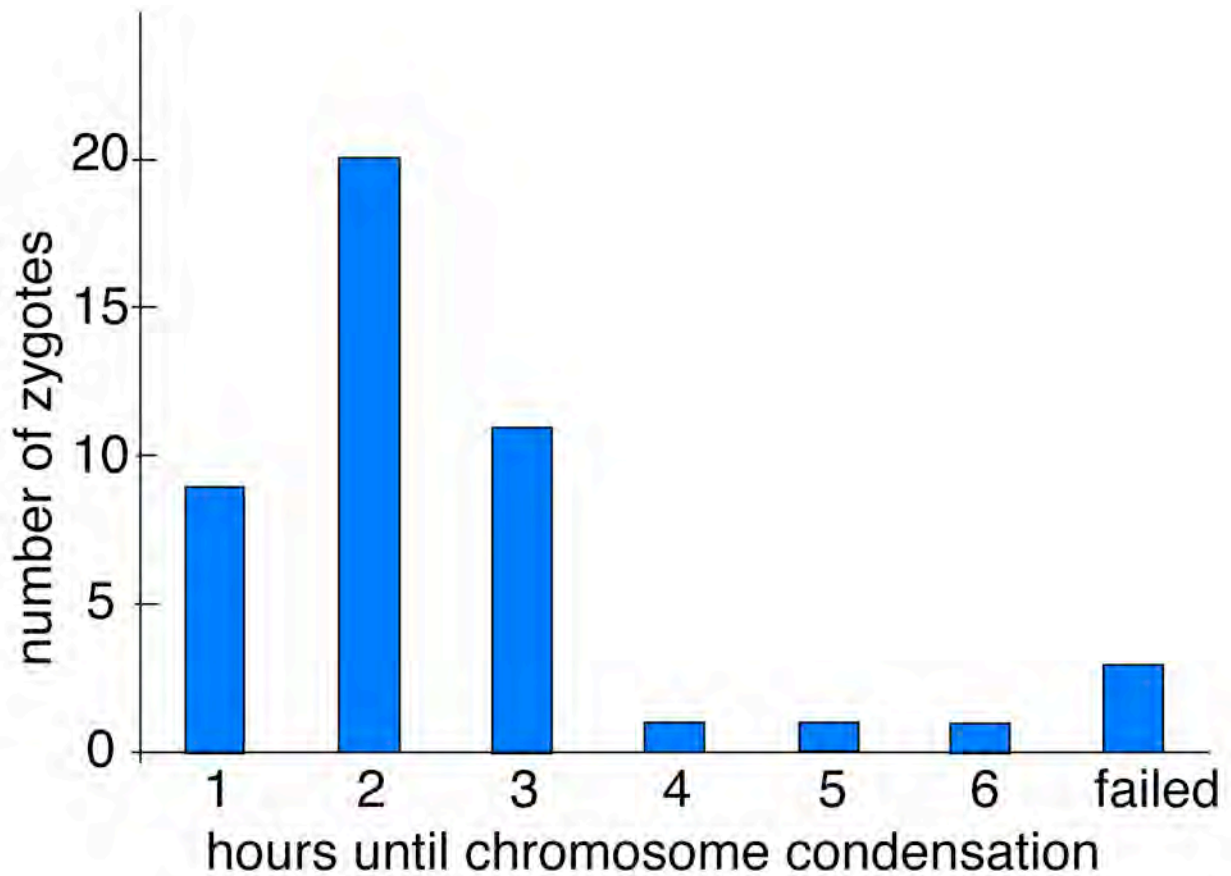
Supplementary Figure S6. Cleavage failure after nuclear transfer into human zygotes

a, Schematic of initial nuclear transfer experiments with human zygotes. The question was whether human zygotes can segregate a transferred mitotic genome into two cells. **b**, zygote in mitosis being enucleated, **c**, removed zygotic genome. **d**, mitotic somatic cell (circled) fusing to the enucleated zygote, the arrow points to the mitotic chromosomes. **e**, Arrested nuclear transfer cell, the nucleus is circled. Time is hours after transfer. Scale bar: 25 μ m.



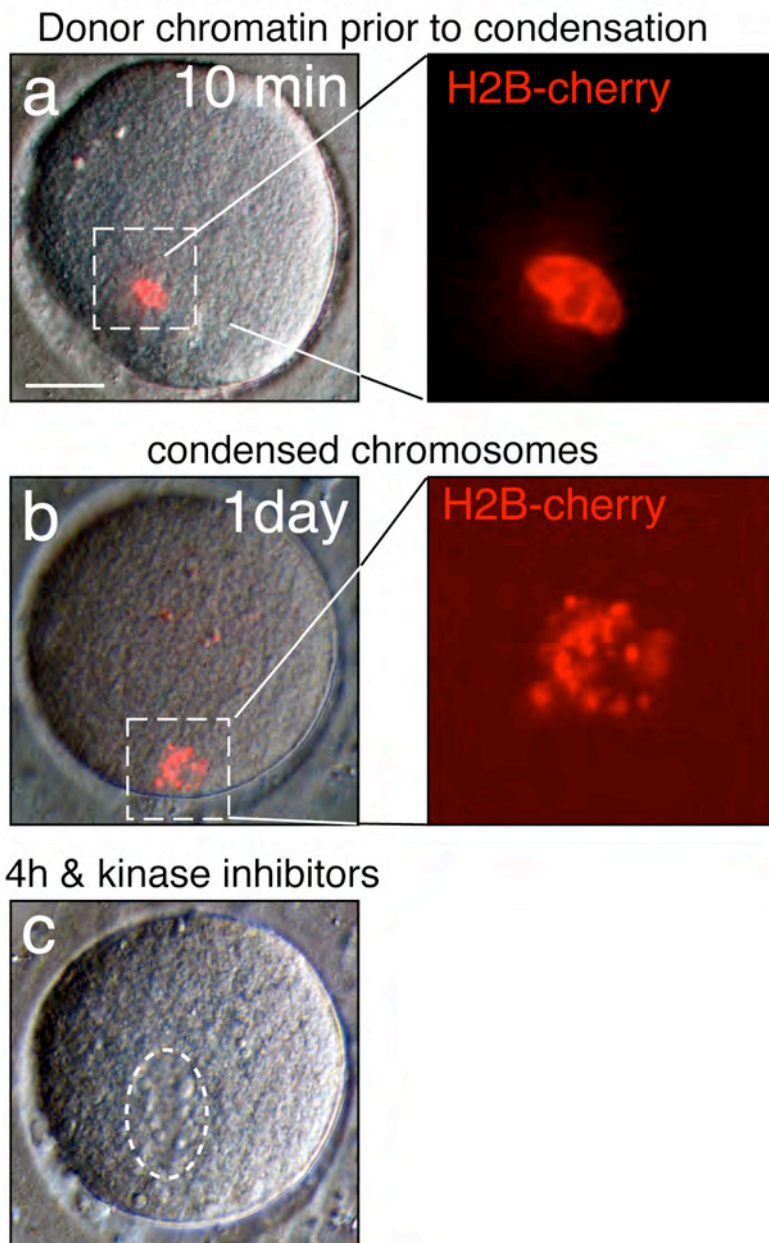
Supplementary Figure S7. Transient nocodazole exposure is compatible with development to the blastocyst stage

Cleavage and development to the blastocyst stage after depolymerization of the spindle by nocodazole at the first mitosis in human zygotes. **a**, schematic representation, **b**, zygote in mitosis imaged by microtubule birefringence. Note that the spindle reassembles after depolymerization by nocodazole. **c**, Cleavage and development to the blastocyst stage. Days indicate the number of days after IVF. Scale bar: 25 μ m.



Supplementary Figure S8. Timing of chromosome condensation after nuclear transfer into human zygotes

Shown is the number of zygotes that had condensed the somatic chromosomes at the indicated time point. Note that chromosome condensation is efficient and occurs in most cases within 3 hours after transfer.



Supplementary Figure S9. Human zygotes do not spontaneously exit mitosis after transfer of a G0 genome

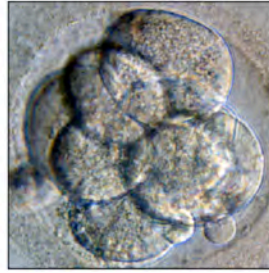
a, Zygote 10min after fusion of a somatic cell nucleus, without removal of the zygotic genome. **b**, 1d after transfer, the cell is arrested at the 1-cell stage, in mitosis. **c**, Addition of kinase inhibitors 6-DMAP and purvalanolA allows entry into interphase. Scale bar: 25 μ m.

developmental stage for array analysis (human)

nuclear transfer



amanitin



IVF

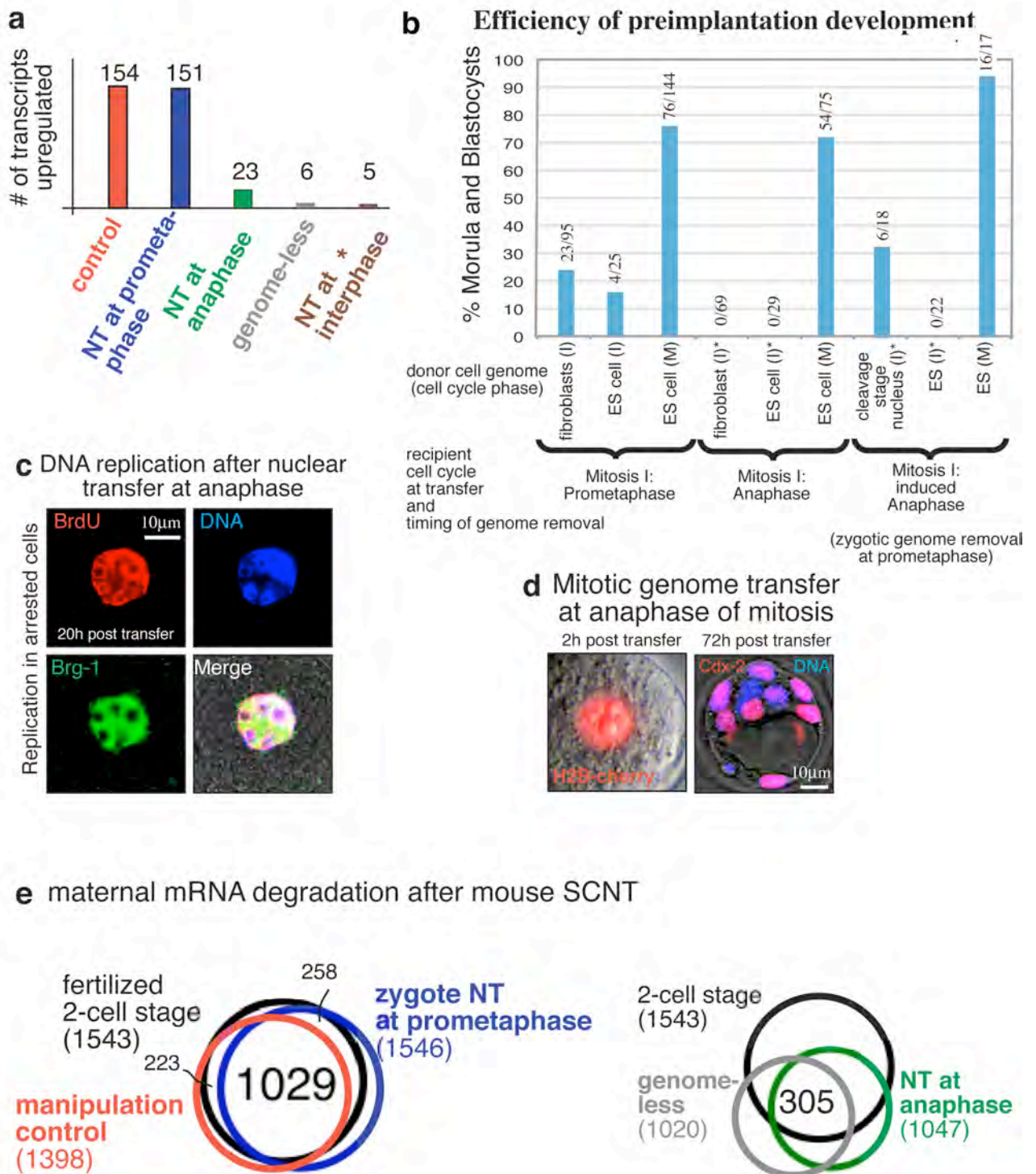


induced aneuploidy



Supplementary Figure S10. Representative samples used for array analysis

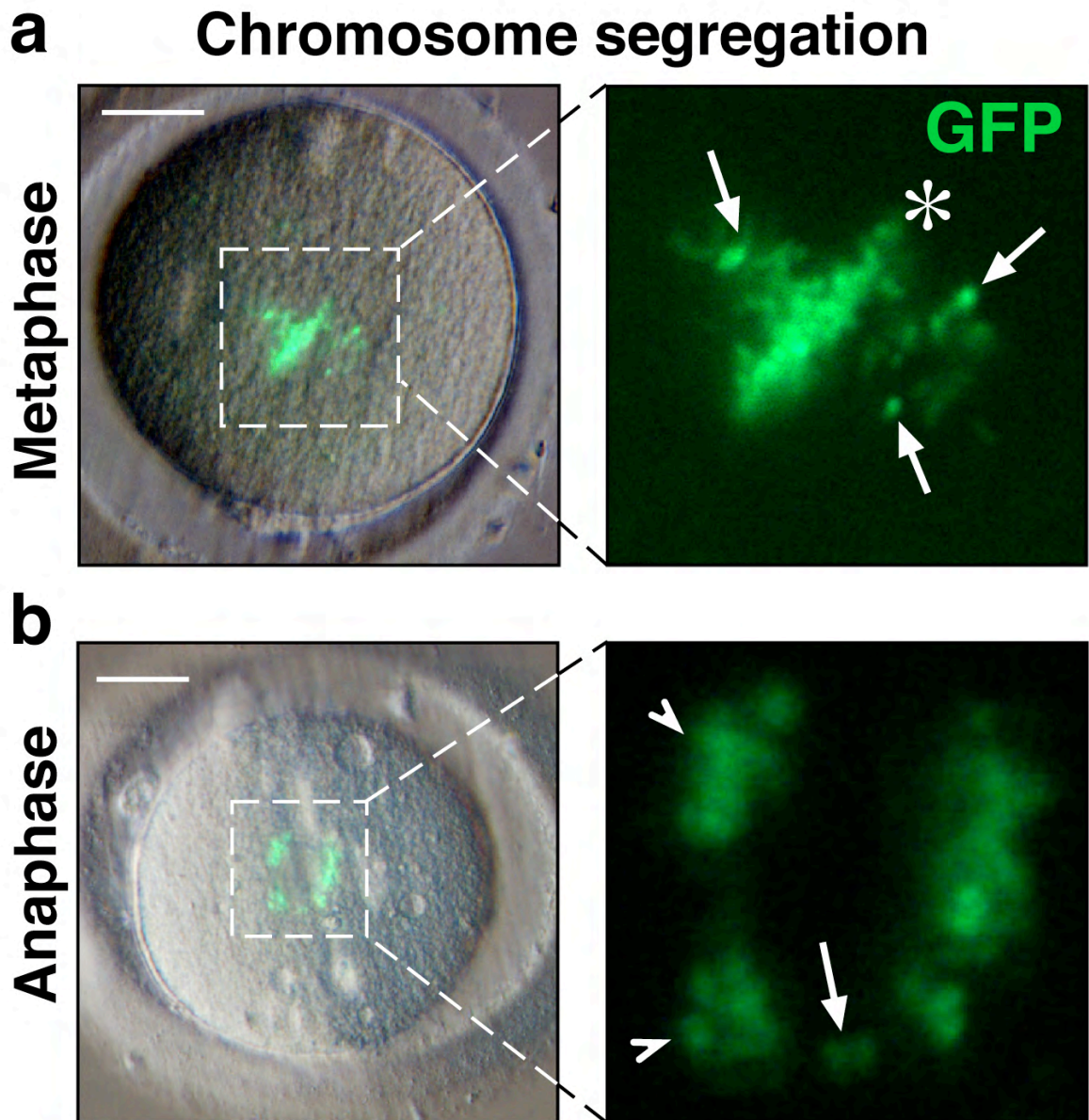
Specimen at the stage used for transcriptional analysis, note equivalent morphological appearance in each group. Scale bar: 25 μ m.



Supplementary Figure S11. Transcriptional reprogramming and development after nuclear transfer into mouse zygotes

a, Upregulation of genes not expressed in the somatic donor cells, and not expressed in M-phase zygotes. Controls are zygotes exposed to drugs as used after nuclear transfer. *NT at interphase data taken from ref. 31. **b**, Efficiency of development to the morula and blastocyst stages. Anaphase zygotes were obtained by release from nocodazole arrest or by inhibition of mitotic kinases (induced anaphase) * Chromosome condensation is inefficient or does not occur under the conditions marked with a star. Numbers indicated the number of morulas and blastocysts of successfully transferred (cleaved) zygotes. Detailed results are presented

in Supplementary Table S3. **c**, Despite developmental and transcriptional arrest after nuclear transfer at anaphase, Brg-1, that is involved in zygotic genome activation⁵⁷, localizes to the nucleus. Replication is also initiated, indicating that cell cycle arrest occurs at S phase or G2 phase. Embryos never progressed to the next mitosis. **d**, mitotic genome transfer of an ES cell into anaphase zygotes rescues developmental potential. The nucleus is immediately remodeled to an embryonic morphology, and development to the blastocyst stage occurs. Cdx2 expression indicates transcriptional reprogramming. **e**, maternal mRNA degradation in fertilized controls, manipulation controls, genome-less cells, and after nuclear transfer into mitotic mouse zygotes at prometaphase or at anaphase. The number of total transcripts downregulated for each group is given in parenthesis. Samples were harvested 22-24h post transfer or post mitosis. Differential regulation was defined as <0.2x change average signal between zygotes and the indicated groups, $p < 0.01$.

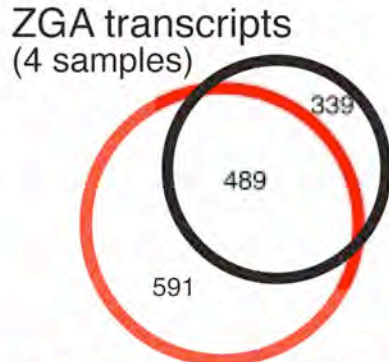


Supplementary Figure S12. Defects in chromosome segregation after nuclear transfer into human zygotes

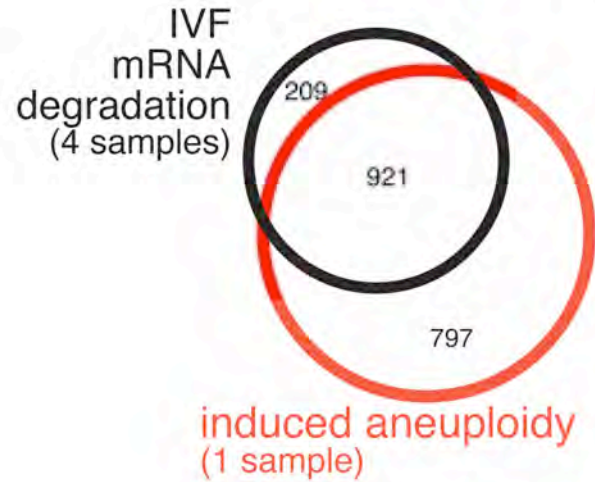
Transfer was done as in Figure 2 with inhibition of the first cytokinesis. The second embryonic mitosis is shown. **a**, Nuclear transfer cell at metaphase of mitosis. The star indicates the metaphase plate and the arrows unincorporated chromosomes. **b**, Nuclear transfer cell at anaphase, arrow points to a lagging chromosome, arrowheads point to separation of a chromosome complement into two groups, resulting in multinucleation. Scale bar: 25 μ m.

gene expression in aneuploid blastomeres (human)

upregulation of zygotic transcripts



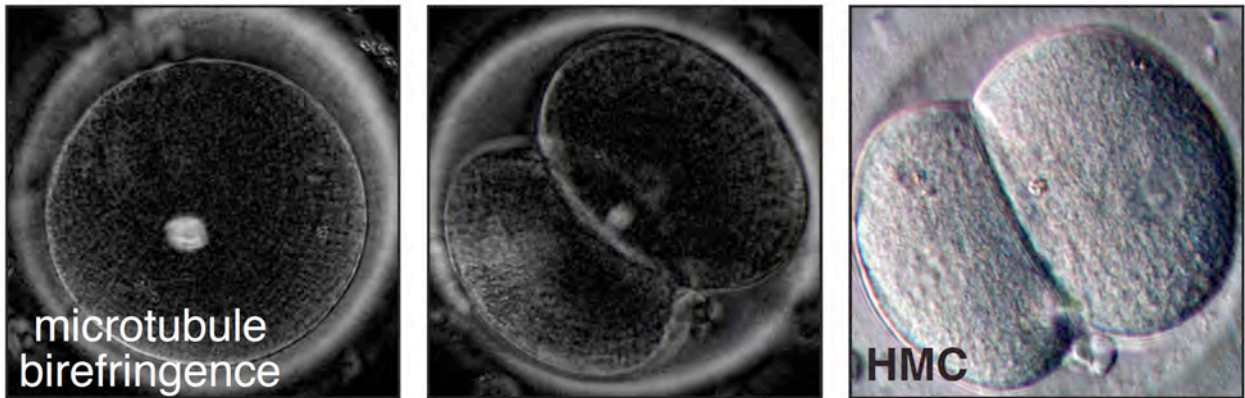
maternal mRNA degradation



Supplementary Figure S13. ZGA and maternal mRNA degradation in aneuploid human embryos

Upregulation of zygotic transcripts and maternal mRNA degradation in after induced aneuploidy (n=1 sample, n=2 specimen of 3 and 5 cells, >5 fold upregulation or <0.2-fold downregulation down-regulation compared to a 1-cell zygote, $p < 0.001$).

4 μ g/ml nocodazole 1h + nocodazole

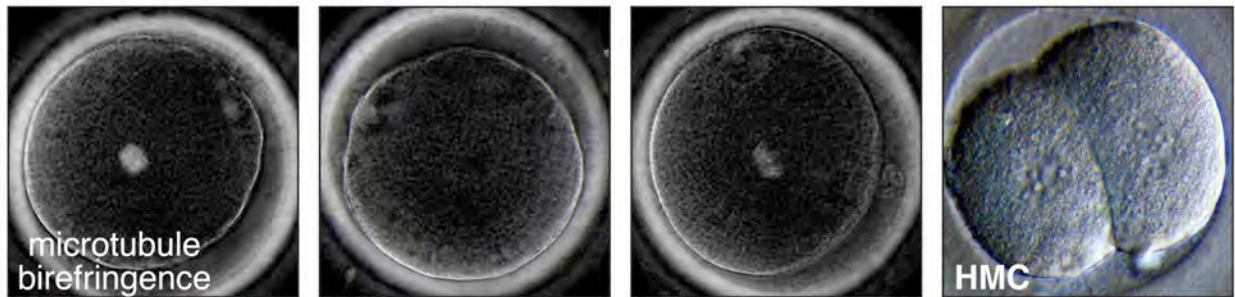


Supplementary Figure S14. Low nocodazole concentrations fail to inhibit progression of human zygotes through mitosis

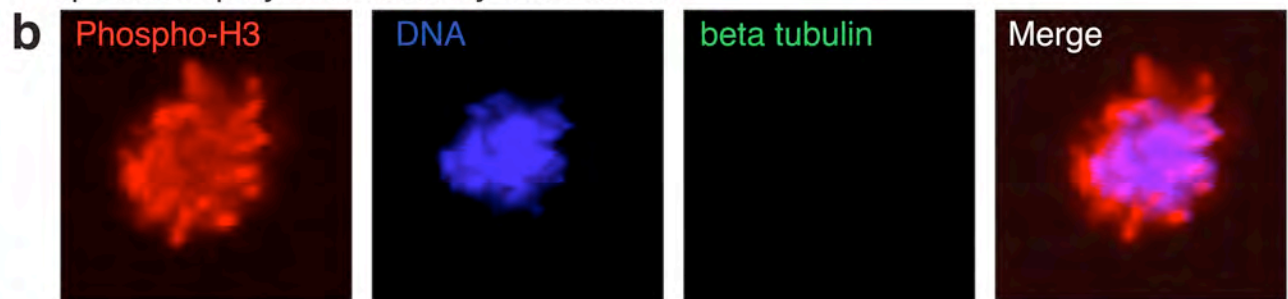
Human mitotic zygote in the presence of 4 μ g/ml nocodazole for 40 min. After 70min, the zygote is cleaving. HMC: Hoffmann modulation contrast.

Effect of vinblastine on human mitotic zygotes

a before drug addition 2min + vinblastine 4.5h - vinblastine



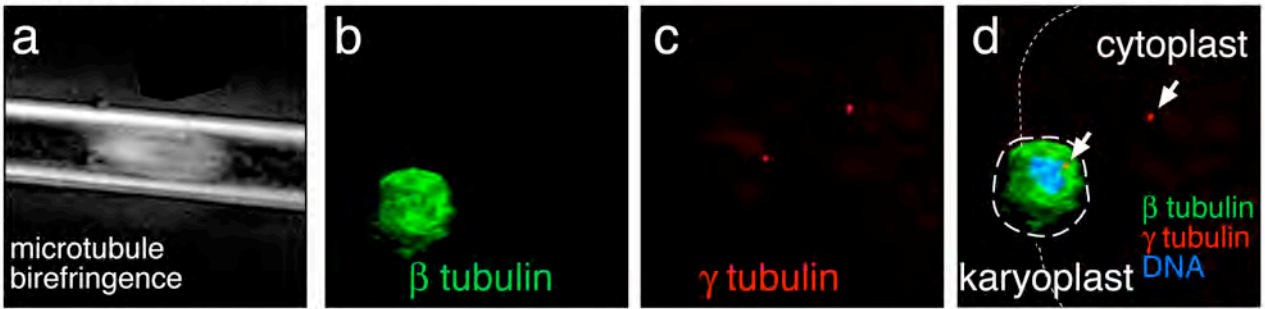
spindle depolymerization by vinblastine



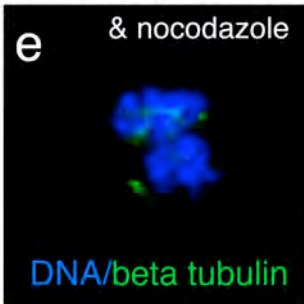
Supplementary Figure S15. Reversible spindle depolymerization by vinblastine in human zygotes

a, Mitotic zygote before drug addition, 2 min after addition of 1 μ M vinblastine, 4.5h after removal of vinblastine, and cleavage to 2 cells. **b**, Immunohistochemistry of a mitotic zygote exposed to 1 μ M vinblastine. Note that virtually no β -tubulin is associated with the chromosomes. HMC: Hoffmann modulation contrast.

aspirated karyoplast

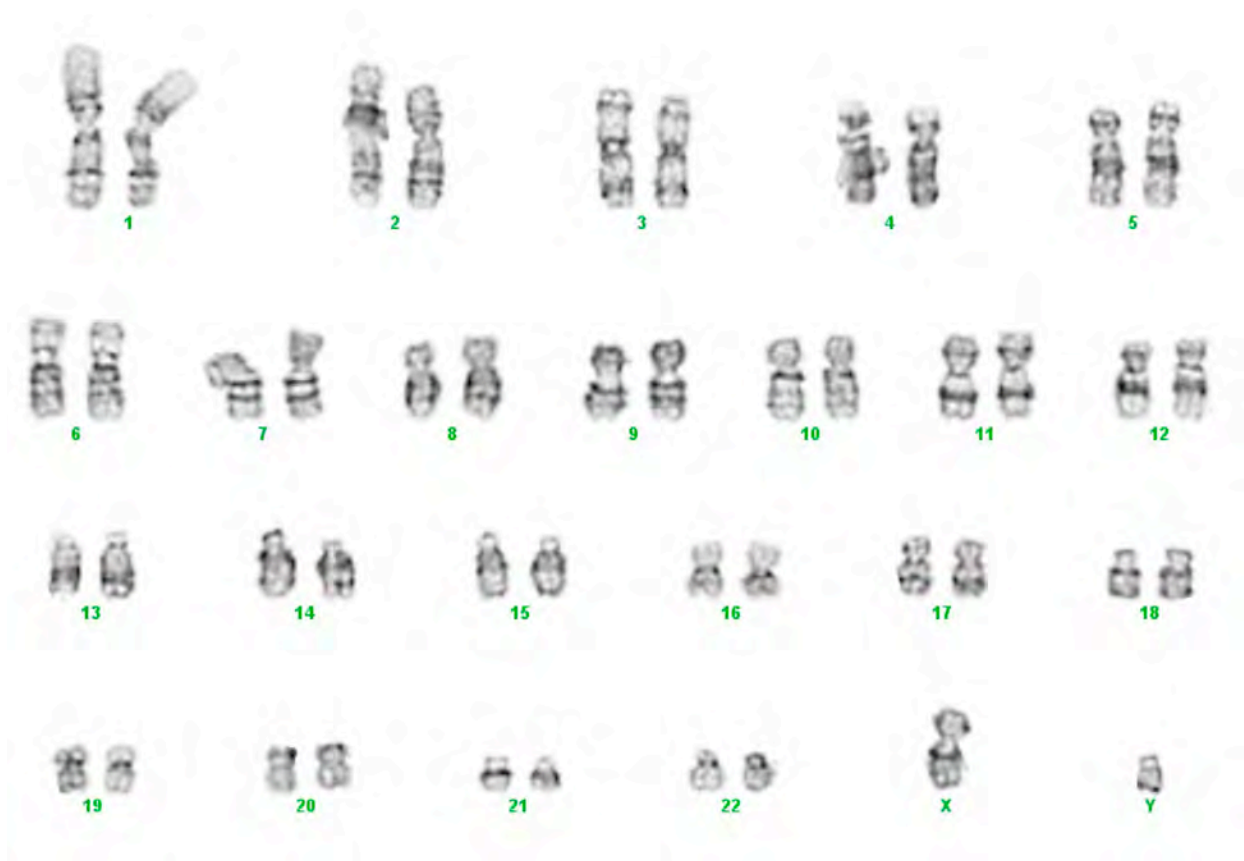


karyoplast



Supplementary Figure S16. Removal of spindle material with the zygotic human genome

Spindle material is removed with the human zygotic genome. **a**, Spindle in the aspiration pipette. **b-d**, immunofluorescence. All resulting cells arrest at the next mitosis with abnormal spindles, despite inhibition of the first cytokinesis after somatic cell genome transfer (18/18). Arrow points to a centrosome that was not removed with the zygotic genome. The dotted lines indicate the boundary of the zygote or the karyoplast. **e**, Nocodazole addition (50 μ g/ml) prior to mitotic entry decreases removal of spindle components. Zygotic genome removed after inhibition of spindle assembly by incubation into nocodazole at the 2PN stage.



Supplementary Figure S17. Karyotype of the somatic donor cell line

This cell line of an adult T1D male was used for nuclear transfer. It has a normal karyotype (46XY).

Supplementary Tables

Supplementary Table S1. Developmental potential after nuclear transfer, and of parthenotes, and zygotes developing in α -amanitin, or other control conditions. The first row (mitotic removal of spindle material). The number indicated under category 'cleaved' consists of the number of zygotes that developed beyond that stage and of the zygotes that arrested after the first cleavage. All cells are human. * only one of the two had the somatic cell genome segregated to the two blastomeres. 12 zygotes used for nuclear transfer are not included in this table because of a failure to complete manipulations properly.

Type of cell/source	Manipulation	Total #used	Total # survived	1-cell arrested	fragmented	cleaved	4-6 cell	7-8 cell	Blastocyst
Zygote	None (control)	28	28	8	2	18	4	4	9
Zygote	Spindle retransfer	10	5	1	2	2	1	-	-
Zygote	Somatic cell transfer without enucleation	15	11	7	2	2*	1	-	-
Zygote	Nuclear transfer	30	8	8	-	-	-	-	-
Zygote	Nuclear transfer (inhibition of cleavage)	15	8	8	-	-	-	-	-
Zygote	Nuclear transfer (nocodazole at 2PN stage, inhibition of cleavage)	69	53	17	3	33	16	7 (2 compacted)	-
Zygote	alpha-amanitin	23	23	-	1	22	14	4	-
Zygote	Inhibition of first cleavage (tetraploid)	17	17	6	2	9	3	2 (1 compacted)	-
Zygote	Electrical pulse in mitosis (control)	4	4	nd	nd	nd	nd	nd	1
Polyspermic zygote	None (control)	7	7	2	1	4	1	3 (2 compacted)	-
Polyspermic zygote	Nuclear transfer	9	9	4	1	2	2	-	-

Supplemental Table S2. Cryopreserved mouse zygotes are suitable recipients for mitotic genome transfer.

Transferred	Cleaved	Morula & Blastocysts
28	18	8 (41% of cleaved)

Supplementary Table S3. Developmental potential after nuclear transfer into mouse oocytes and zygotes.

I, interphase; M, mitosis; A, Anaphase of mitosis; zyg, zygote; PS, pluripotent stem cell (ESC); 8-12 cell: blastomeres. * shows the number of cells with interphase nuclei in the first interphase after transfer and inhibition of cytokinesis. G1: interphase synchronized by release from mitotic nocodazole arrest for 1h. N/A: not applicable. P/D: purvalanol A and 6-DMAP.

recipient (cell cycle stage at transfer)	donor (cell cycle stage)	recipient genome removal	# manip	First interphase	Second interphase	morulae d3.5	blastocysts d3.5	morulae & blastocysts % of cleaved
zyg (M)	fibroblast (I)	Prometaphase	324	95* (29)	ND	14	9	24
Zyg (A)	Fibroblast (I)	Anaphase	108	69* (64)	0	0	0	0
Zyg (M)	PS (M)	Prometaphase	168	144 (85)	ND	28	82	76
Zyg (M)	PS (I)	Prometaphase	46	25* (54)	ND	2	2	16
Zyg (A)	PS (I)	Anaphase	61	29* (47)	1	0	0	0
Zyg (A)	PS (M)	Anaphase	110	75* (68)	ND	11	43	72
Zyg (A)	PS (T)	Anaphase	3	2* (66)	ND	1	1	N/A
Zyg (M, & P/D)	PS (I)	Prometaphase	36	22* (61)	4	0	0	0
Zyg (M, & P/D)	PS (M)	Prometaphase	25	17* (68)	ND	3	13	94
Zyg (M, & P/D)	8-12 cell (I)	Prometaphase	42	18* (42)	11	4	2	33
oocyte (MII)	PS (M)	meiosis	19	12 (63)	ND	2	4	50
oocyte (MII) activated	PS (M)	meiosis	56	31 (55)	ND	7	20	87
oocyte (MII)	PS (I)	meiosis	76	40* (52)	ND	0	12	30
oocyte (MII) activated	PS (I)	meiosis	81	53* (65)	ND	2	2	7
oocyte (MII)	Fibroblast (I)	meiosis	98	58* (60)	ND	10	6	27

Supplementary Table S4. Karyotypic abnormalities in nuclear transfer blastomeres and blastomeres from IVF specimen. White and purple columns are the experimental data. White columns: not all blastomeres had these chromosomes determined. All cells are human.

IVF specimen	13	16	18	21	22	14	15	17	X	Y
1	3	3	3	3	3	nd	nd	nd	nd	nd
1	0	1	1	0	2	nd	nd	nd	nd	nd
2	5	6	5	5	5	nd	nd	nd	nd	nd
2	2	2	2	2	2	2	1	2	2	0
2	2	2	2	1	2	2	2	2	2	0
3	3	2	2	2	2	2	2	2	1	1
3	2	2	2	2	2	0	2	0	1	0
3	2	2	3	2	2	1	2	1	2	1
3	0	2	2	2	2	nd	nd	nd	nd	nd
3	0	2	1	2	2	2	2	2	1	1
3	2	2	2	2	2	2	2	2	1	1
3	2	2	2	2	2	1	3	2	2	1
3	1	2	3	2	1	2	2	2	1	1
	2	2	1	2	2	0	3	0	1	2
4	4	4	4	4	4	4	4	4	4	0
4	2	1	1	2	0	2	1	2	2	0
4	5	4	4	4	4	0	4	4	4	0
4	2	2	2	2	2	2	2	2	2	0
5	2	2	2	2	2	2	2	2	1	1
5	2	2	2	2	2	nd	nd	nd	nd	nd
6	5	4	4	5	3	4	4	4	3	1
6	2	4	4	2	6	3	2	2	3	0
6	2	1	3	2	2	nd	nd	nd	nd	nd
zygote SCNT	13	16	18	21	22	14	15	17	X	Y
1	2	nd	2	1	nd	nd	nd	nd	0	1
1	1	nd	2	1	nd	nd	nd	nd	1	1
1	2	nd	0	2	nd	nd	nd	nd	1	1
2	2	nd	1	1	nd	nd	nd	nd	1	1
2	1	nd	1	0	nd	nd	nd	nd	1	1

Supplementary Table S5. Bipolar and multipolar cleavage in tetraploid human zygotes and after nuclear transfer.

The variation in the expected number of centrosomes is due to the uncertainty in removing the zygotic centrosomes with the zygotic genome. Nd= not determined.

Type of cell (expected number of centrosomes)	Total	Arrested at 1-cell stage	Fragmented	Cleavage to 2 cells	Cleavage to 3 cells	Cleavage to 4 cells	nd
2PN zygote (2)	28	7	2	18	-	-	-
Polyspermic zygote (3 or more)	7	2	1	1	3	-	-
Tetraploid zygote (4)	17	6	2	2	3	4	-
NT into polyspermic zygotes (2-6)	8	3	1	-	2	2	-
NT into 2PN zygotes (2-4)	53	17	3	11	5	3	14

Supplemental Table S6. Bipolar cleavage in mouse and rabbit tri- and tetraploid zygotes

Cell Type	Total	Cleaved to 2-cell	Blastocysts
Polyspermic mouse zygote	18	14 (4 are arrested at 1-cell stage)	14
Tetraploid mouse zygote (inhibition of cytokinesis at first mitosis)	19	17	16
Tetraploid rabbit zygote (inhibition of cytokinesis at first mitosis)	8	8	8

Supplemental Table S7. Effective nocodazole and vinblastine concentrations in human zygotes. Nocodazole. n/a: not applicable. * cleavage only after release from vinblastine or nocodazole. At lower concentrations cleavage occurs in the presence of nocodazole.

Number of zygotes	Microtubule inhibitor	Time point of drug application	Spindle assembly	# of zygotes that underwent cleavage	Development	Cell line
6	2 µg/ml nocodazole	2PN	Yes	n/a	n/a	n/a
3	2 µg/ml nocodazole	Mitosis	Yes	3	1 blastocyst 2 morula	HUES47 (46XX)
1	4 µg/ml nocodazole	Mitosis	Yes	1	n/a	n/a
13	50 µg/ml nocodazole	Mitosis	No, spindle de-polymerization	10*	1 blastocyst	-
4	1mM Vinblastine	Mitosis	No, spindle de-polymerization	1*	1 morula	-